Investigation of the Open Ring Form of Nicotinamide Adenine Dinucleotide†

C. C. Guilbert‡ and S. L. Johnson*

ABSTRACT: In strong alkali, nicotinamide adenine dinucleotide (NAD^+) undergoes a ring opening of the nicotinamide ring. The open form of NAD^+, ONAD, has two pK_a values at −1.9 and 11.2 and absorbs maximally at 350 nm in its acidic form, at 372 nm in its neutral form, and at 340 nm in its anionic form. ONAD has the chemical properties expected for a Schiff base of 2-carboxamideglutacondialdehyde (CGDA) and adenosine diphosphate ribosylamine. The decomposition of ONAD has been studied over a wide range of pH. A final product of ONAD hydrolysis is the base fluorescent compound 2-hydroxynicotinaldehyde. In the pH range 10–13, CGDA can be trapped as an intermediate, which absorbs maximally at 345 nm in its anionic form and at 320 nm in its neutral form, pK_a = 2.9. The yield of 2-hydroxynicotinaldehyde from ONAD has been estimated as 95% at NaOH concentrations of 5 N and above, and is postulated to result from ring closure of CGDA. The pseudobase hydroxide ring addition adduct of NAD^+, ψNAD-OH, is reversibly formed from NAD^+ and is the 370-nm precursor of ONAD.

A number of dehydrogenases facilitate the formation of ternary complexes with NAD^+ [1] and nucleophiles. These ternary complexes absorb maximally in the near-ultraviolet in the range of 300–400 nm. Examples are: addition of cyanide and pyruvate by lactate dehydrogenase (Fromm, 1961; Everse et al., 1971; Gerlach et al., 1965); addition of hydroxylamine and cyanide by alcohol dehydrogenase (Kaplan et al., 1954); and addition of mercaptans by a number of dehydrogenases (Van Eys et al., 1958). Addition of nucleophiles to NAD^+ occurs in the absence of enzyme. These addition complexes are, in the case of lactate dehydrogenase, the result of addition of the nucleophile to the 4 position of NAD^+ (Arnold and Kaplan, 1974; Adams et al., 1973). Kaplan and Everse (1972) have proposed that the ternary complex formed with NAD^+, pyruvate, and lactate dehydrogenase plays a role in metabolite regulation in the living cell.

The binding of NAD^+ to the enzyme glyceraldehyde-3-phosphate dehydrogenase produces an absorption band around 365 nm, which has been variously attributed to a mercaptan addition (Racker and Krimsky, 1952) and to a charge-transfer complex between NAD^+ and a tryptophan or cysteine residue (Kosower, 1962). Recent x-ray structural studies rule out the involvement of a tryptophan group (Buehner et al., 1974). Lactate dehydrogenase also forms a chromophoric complex with NAD^+ (Vestling and Kunsch, 1968).

Another type of nucleophilic reaction with NAD^+ which yields chromophoric products has recently been found, that is, ring opening following addition. NAD^+ has been postulated to undergo ring opening of the nicotinamide ring in strongly alkaline solutions (Johnson and Morrison, 1970a). A transient intermediate, ψNAD-OH, absorbing at 370 nm is produced initially (see Scheme I). ψNAD-OH is reversibly formed from

Scheme I

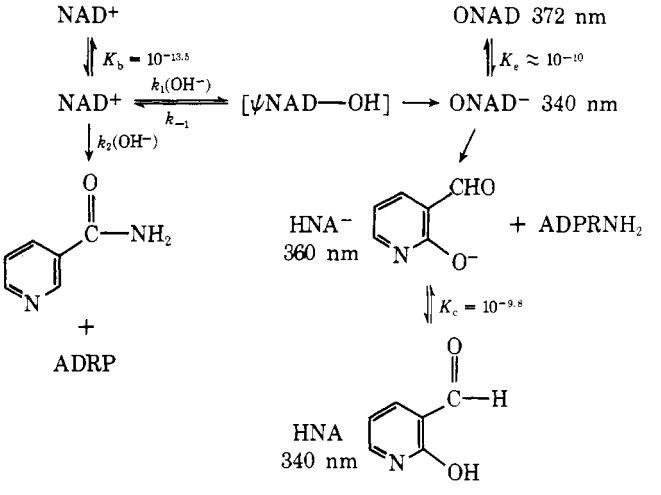

NAD^+ and is converted irreversibly to a 340-nm absorbing species (Johnson and Morrison, 1970b). This 340-nm intermediate, ONAD, absorbs maximally at 372 nm in the buffers below pH 10 and has a pK_a around 10 (Johnson and Morrison, 1970b). ONAD is replaced by a final fluorescent product absorbing at 360 nm in alkaline solution (Kaplan et al., 1951) and has been identified as 2-hydroxynicotinaldehyde (Guilbert and Johnson, 1970). 2-Hydroxynicotinaldehyde, HNA, absorbs at 340 nm in acidic solution and has a pK_a of 9.8. HNA is also produced from the alkaline ring opening of 1-(*N,N*-dimethylcarbamoyl)nicotinamide chloride, DCN (see Scheme II)

† From the Department of Biochemistry, University of Pittsburgh, School of Medicine, Pittsburgh, Pennsylvania 15261. *Received December 31, 1975.* This work was supported by Public Health Service Grant GM16856.

‡ This work is from a dissertation submitted in partial fulfillment of the requirements for the degree of Doctor of Philosophy in the Graduate Program of Biochemistry, University of Pittsburgh, School of Medicine, Pittsburgh, Pennsylvania 15261.

[1] Abbreviations used: NAD^+, nicotinamide adenine dinucleotide; Tris, 2-amino-2-hydroxymethyl-1,3-propanediol; OD, optical density; ψNAD-OH, the hydroxide ring addition adduct pseudobase of NAD^+; ψNAD-O^-, the conjugate base of ψNAD-OH; ONAD, the ring-opened form of NAD^+; $ONAD^-$, the conjugate base of ONAD; $ONAD^+$, the conjugate acid of ONAD; HNA, 2-hydroxynicotinaldehyde; HNA^-, conjugate base of HNA; DCN, *N,N*-dimethylcarbamoylnicotinamide cation; ODCN, the ring-opened form of DCN; DCP, *N,N*-dimethylcarbamoylpyridinium ion; ODCP, the ring-opened form of DCP; ADPR, adenosine diphosphoribose; CGDA, 2-carboxamideglutacondialdehyde; GDA, glutacondialdehyde (2,4-pentadiene-1,5-dial); NAD^+, NAD^+ ionized at the amide group; Tris, tris(hydroxymethyl)aminomethane.

Scheme II

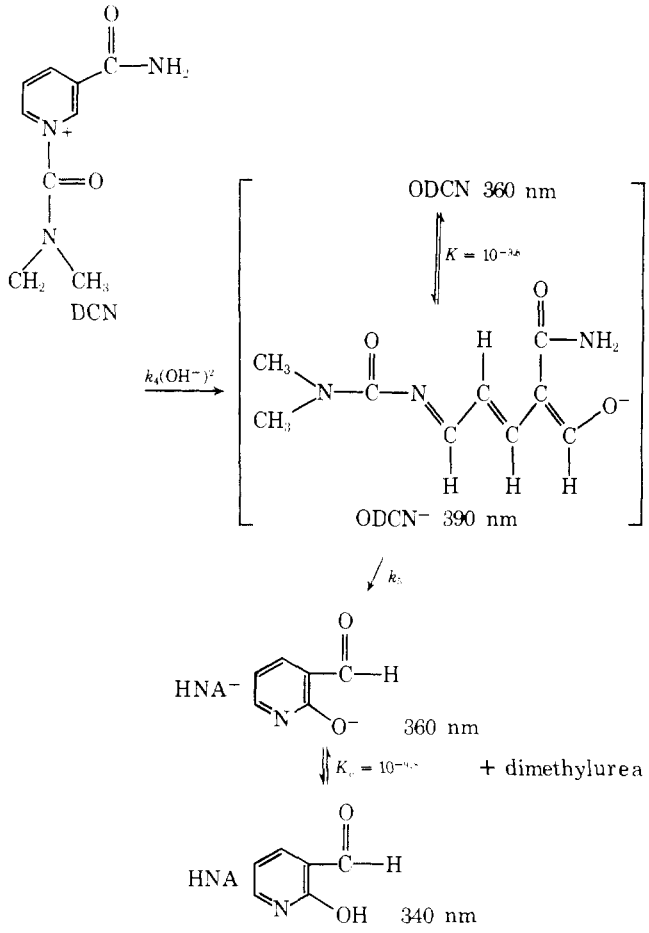

(Guilbert and Johnson, 1970). The initally formed ring-opened species, ODCN, is produced by a reaction second order in hydroxide ion at pH values above 7, has a pK_a of 9.8, and absorbs maximally at 393 nm in its anionic form and at 360 nm in its neutral form.

In order to elucidate the 340-nm alkaline modification of NAD^+, its properties were investigated and the nature of its decomposition was determined at a wide range of pH values. The results are consistent with a ring-opened structure, ONAD, indicating nucleophiles with two replaceable hydrogens can produce ring opening of the nicotinamide ring of NAD^+. This may have important implications in the binding of NAD^+ by dehydrogenases.

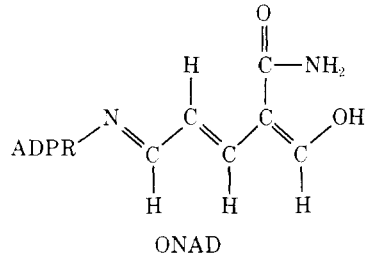

Experimental Section

Materials

NAD^+ was a product of Sigma Biochemicals. Neurospora NAD^+ nucleosidase and yeast alcohol dehydrogenase were products of Worthington Biochemicals. Buffers were prepared from reagent-grade chemicals.

Methods

Chromatography. Thin-layer chromatography was carried out with silica gel or cellulose plates containing fluorescent indicator. Compounds were located after development by examination under white light or both short and long wavelength ultraviolet light, or by examination after spraying with either 0.5% 2,4-dinitrophenylhydrazine in 2 N HCl or with 1.2% aniline *o*-phthalate, 1% epichlorohydrin aerosol. Solvents used for chromatography were (A) 60% acetone, (B) 67% pyridine, and (C) water-saturated 1-butanol.

pH Determinations. Determinations at acid pH values were made in HCl solutions and H_0 values were used to express the pH (Paul and Long, 1957). For runs made at pH > 13, H_- acidity functions were used (Yagil, 1967). All other pH values were directly measured using a Radiometer TTT-1 pH meter. Alkaline solutions were corrected for electrode error. At pH values of 0.4–13.4, the ionic strength was maintained at 0.6 M with KCl.

pK_d and pK_e of ONAD and pK_f of CGDA. The pK_d and pK_e of the opened ring were determined by adding identical aliquots of a 0.01 M solution of ONAD to identical amounts of buffer solution of various pH. The optical density at 370 nm, measured on a Beckman DU spectrophotometer thermostated at 25.0 ± 0.01 °C, was read as a function of time and the initial optical density was obtained by extrapolation to zero time on an optical density vs. time plot. The pK_e value is equal to pH + log $[(d_i - d)/(d - d_u)]$, where d_i refers to the optical density of the completely ionized molecule measured at high or low pH values, d refers to the optical density at intermediate pH values (pH 10–12), and d_u refers to the optical density of the neutral form measured at pH values near neutrality. pK_f was determined by placing aliquots of CGDA (obtained by prior incubation of ONAD in 0.1 N NaOH for 1 h) in buffers of different pH. A precise determination of pK_f was not possible because of the instability of GCDA, which decomposes 10% in 1 h at 0 °C.

Quenching Method for Following Appearance and Disappearance of the 340-nm Intermediate ONAD from NAD^+. An aliquot, 0.05 ml of 0.05 M NAD^+, was added to 2 ml of 5 N NaOH for various periods of time. This mixture was cooled in a −20 °C bath for 15 s before acid quenching with 0.3 M Tris-HCl and 7.9 M HCl, which brings the final pH to around 8.2. The absorbance of the quenched solution at 370 nm was determined. An end point solution was quenched after incubation overnight.

A similar sequence was carried out for 2.5, 1, and 0.5 N NaOH, adjusting the amount of NAD^+ added, and the volumes of NaOH and acid-quench mixture were used as necessary to obtain a final pH of 8.2 and sufficient absorbance at 370 nm for good kinetic determination. The quenching method could not be used at NaOH concentration greater than 5 N because of heating problems which destroyed the 370-nm absorbance.

Fluorescence Kinetic Studies of 2-Hydroxynicotinaldehyde Formation from NAD^+ and from ONAD. An Aminco-Bowman spectrofluorimeter was used with excitation at 360 nm and emission at 460 nm. An aliquot of NAD^+ or ONAD was added to 3 ml of the appropriate NaOH concentration in a cuvet. The fluorescence of the solution was read at various time intervals, and the cuvet was kept at an ambient temperature of 25–26 °C outside the fluorimeter between readings.

The stability of 2-hydroxynicotinaldehyde in 7.5 and 10 N NaOH was checked under the conditions used for the kinetic measurements, since this compound is known to be photolabile in strongly alkaline solutions (Kaplan et al., 1951). A fluctu-

ation of 2% in readings was observed for the fluorescence, with the final fluorescence being essentially the same as the initial readings. Under the conditions of the experiment, 2-hydroxynicotinaldehyde is stable.

The fluorescence measured at 460 nm after excitation at 360 nm is not due exclusively to production of 2-hydroxynicotinaldehyde from NAD^+, since completed reactions of NAD^+ in 1, 2.5, and 5 N NaOH, showed at least three other blue fluorescent spots after spraying with 0.1 N NaOH, following chromatography in solvents A and B. These other blue fluorescent spots were also blue fluorescent below pH 9. The acid form of 2-hydroxynicotinaldehyde is not fluorescent.

Preparation of ONAD. NAD^+, 1.25 g, was dissolved in 1 ml of water and 4 ml of 5 N NaOH was added with stirring. After 3.75 min, the mixture was immersed in a −21 °C bath and the reaction was quenched at 4 min with 2.4 ml of 0.3 M Tris-HCl, 8.0 M HCl. After 1 min, an aliquot of the solution was checked for NAD^+ content by alcohol dehydrogenase assay (Klingenberg, 1965). If NAD^+ was present, the solution was treated with *Neurospora* NAD^+ nucleosidase until all NAD^+ was destroyed. Water was removed either by lyophilization or by evaporation in vacuo. The residue was extracted with 5 ml of water, filtered to remove NaCl, and added slowly with stirring to 50 ml of absolute ethanol. The solvent was decanted off and the gummy precipitate was dissolved in 5 ml of water. The precipitation procedure was repeated twice. The resulting yellow precipitate was dried over calcium chloride. For further purification, 500 mg of the yellow powder was dissolved in 1 ml of water and streaked onto several preparative thin-layer cellulose plates. After development with solvent A, the streak, which absorbed long-wave ultraviolet light, was scraped from the plates and extracted with 80 ml of water. After lyophilization, a pale yellow powder was obtained. This material contained no NAD^+ by alcohol dehydrogenase assay and was used for kinetic determinations and for the chemical characterizations. The insolubility of this material in organic solvents and its lability of acidic and basic pH values limited the methods of purification. Thin-layer analysis using solvent B showed the material contained several impurities. In this system, ONAD had an R_f value of 0.79, and gave an orange color with aniline phthalate. The impurities had R_f values of 0.71, 0.60, 0.51, and 0.45; the first three correspond to adenosine diphosphate ribose, adenosine diphosphate, and adenosine monophosphate, respectively. The purity of ONAD was estimated as 33% (see Results). The optical properties of ONAD at various pH values were obtained by extrapolation to zero time.

Kinetic Studies of ONAD. The rate of disappearance of ONAD ($0.5\text{–}1.0 \times 10^{-5}$ M) was determined spectrophotometrically at 370 nm below pH 12, and at 340 nm above pH 12, using a Beckman DU-2 spectrophotometer thermostated at 25.00 ± 0.01 °C. All rate constants, except for the run in the pH 7.2 Tris buffer, were corrected for buffer catalysis by extrapolation to zero buffer concentration using a series of five successive dilutions of the stock buffer of known composition.

Kinetic Studies of 2-Carboxamideglutacondialdehyde, CGDA. A stock solution of CGDA was prepared by incubation of 20 mg of ONAD in 0.2 ml of 0.1 N NaOH for 1 h. Rate constants for the decomposition of CGDA in the pH region 13–16.2 were obtained by following the decrease in absorbance at 345 nm on a Cary 14 spectrophotometer at 26 ± 1.5 °C after introduction of an aliquot of CGDA into the appropriate buffer. Completed reactions were scanned for absorbance to determine the final product of decomposition.

Yield of 2-Hydroxynicotinaldehyde from ONAD. The yield of 2-hydroxynicotinaldehyde from ONAD as a function of NaOH concentration was determined by measurement of the absorbance at 360 nm after incubation of 0.762×10^{-4} M ONAD in the appropriate NaOH solution until no further change in the ultraviolet spectrum occurred. The percent yield was calculated using a value of 8000 M^{-1} cm^{-1} for the extinction coefficient at 360 nm of 2-hydroxynicotinaldehyde.

Product Studies of the Decomposition of ONAD. Spectral scans of completed reactions were performed on a Cary 14 spectrophotometer. In order to test for ring closure of ONAD to form NAD^+, separate 20-mg samples of ONAD were incubated for 2 h in 0.01 ml of 3 N HCl, pH 11.5, phosphate buffer, 0.1 N NaOH, and 5 N NaOH. Similar samples were also incubated for 1 h. Aliquots of each incubation mixture were assayed for NAD^+ using alcohol dehydrogenase (Klingenberg, 1965). The sample size added, 0.01 ml, was sufficient to detect easily NAD^+ produced in a yield of 10%. Inhibition of the enzyme, checked by adding NAD^+ to each assay mixture, was shown not to occur. Aliquots of each incubation were neutralized and spotted onto two cellulose thin-layer chromatographic plates, which were separately developed with solvents A and B.

Results

Kinetic Studies on the 340- and 360-nm Intermediates from NAD^+. The rates of formation and decomposition of the 340-nm intermediate, ONAD, and the rates of formation of 2-hydroxynicotinaldehyde from NAD^+ are given in Table I. The rate constants for formation of ONAD from NAD^+ increase with increasing NaOH concentrations to a maximal value at 2.5 N NaOH and then subsequently decline at higher NaOH concentrations. Similarly, the rate constants for disappearance of ONAD increase with increasing NaOH concentration to a maximum value at 1 N NaOH and then subsequently decline at higher NaOH concentrations. The difference of 25–55% between the values of the rate constants obtained by the acid quench and direct spectral method is probably due to the experimental error involved in both methods. The absorbance at 340 nm reflects a number of species; the 372-nm acid form of ONAD has a higher extinction coefficient and is a better measure of the amount of ONAD present.

Rate constants for the appearance of 2-hydroxynicotinaldehyde from NAD^+ at NaOH concentrations less than 5 N were obtained from good first-order plots of log $(F_\infty - F_t)$ vs. time. At 5 N NaOH and above, the pseudo-first-order plots are biphasic with an initial fast increase in fluorescence, followed by a slower first-order reaction. The rate constants for this initial burst reaction are similar in magnitude to those obtained for the formation of ONAD from NAD^+ and may be due to side reactions of NAD^+ which form fluorescent products. The acid quench solution obtained after 4-min incubation of NAD^+ in 5 N NaOH and also completed reactions in 1, 2.5, and 5 N NaOH showed several other blue fluorescent spots on chromatography in solvents A and B. The amount of fluorescence increase due to the burst region is about the same or less than the amount of side products formed from NAD^+. The rate of decomposition of ONAD and the rate of appearance of 2-hydroxynicotinaldehyde are approximately equal, supporting the postulate that ONAD is transformed to 2-hydroxynicotinaldehyde.

Properties of ONAD and CGDA. The various properties of ONAD were studied using the preparation made as described under the Experimental Section. The purity of ONAD was

TABLE I: Rate Constants for HNA Formation and Formation and Decay of ONAD, the 340-nm Intermediate, from NAD^+.

NaOH (M)	pH[a]	First-Order Rate Constant for ONAD Formation[b] (min^{-1})		First-Order Rate Constant for ONAD Decay[b] (min^{-1})		First-Order Rate Constant for HNA Formation[c] (min^{-1})
		Acid Quench	340 nm	Acid Quench	340 nm	
0.5	13.7	0.50	0.40	0.075	0.033	0.056
1.0	14.0	0.58	0.61	0.089	0.057	0.084
2.5	14.54	0.82	0.82	0.066		0.082
5.0	15.2	0.66	0.82	0.055	0.035	0.063
7.5	15.7		0.57		0.018	0.050
10.0	16.2		0.42			0.037

[a] See Yagil (1967). [b] First column: determined by acid-quench method at 26 °C; second column: determined by measurement at 340 nm and 25 °C, from Johnson and Morrison (1970). [c] Determined by measurement of fluorescence at 26 °C. Burst reactions were observed in 5, 7.5, and 10 M NaOH corresponding to 10, 22, and 31% of the total fluorescence increase, respectively. The percent yield of HNA under these conditions is 77, 78, and 62%, respectively.

estimated as 33% from these considerations. The apparent extinction coefficient of neutral ONAD is 11 200 M^{-1} cm^{-1} for the maximal absorbance at 372 nm, whereas the neutral form of GDA has an extinction coefficient of 34 000 M^{-1} cm^{-1} for its maximal absorbance at 335 nm (Johnson and Rumon, 1970). If the extinction coefficient of ONAD at 372 nm is taken as 34 000 M^{-1} cm^{-1}, a purity of 33% is calculated. After chromatography in solvent B and elution into pH 7.01 phosphate buffer, the impurities absorbed maximally at 260 nm. At 5 N NaOH, the yield of ONAD from NAD^+ is maximal with an apparent extinction coefficient (360 nm) of 1.2×10^4 M^{-1} cm^{-1}. Since the yield of 2-hydroxynicotinaldehyde from NAD^+ is 70% at 5 N NaOH (Guilbert and Johnson, 1970) and if it is assumed that ONAD is completely converted to 2-hydroxynicotinaldehyde, a minimum extinction coefficient at 17 000 M^{-1} cm^{-1} can be calculated for anionic ONAD. The measured extinction coefficient for the isolated preparation of ONAD at 340 nm in 1 N NaOH is 5600 M^{-1} cm^{-1}; the purity of ONAD is therefore calculated as 33% by comparison of the two values. This value is in excellent agreement with the value obtained by assuming a value of 34 000 M^{-1} cm^{-1} at 372 nm for the extinction coefficient of ONAD.

The properties of ONAD are as follows: λ_{max} at 350 nm in very acid solutions; λ_{max} at 372 nm in the pH range 1–10; λ_{max} at 340 nm in very alkaline solutions. Two pK values were determined by spectral methods: −1.90 and 11.18. ONAD yields 2-hydroxynicotinaldehyde at strongly alkaline pH values, as does ODCN (Johnson and Morrison, 1970a). The spectroscopic and acid–base properties of ONAD indicate that its structure is that of a Schiff base of adenosine diphosphate ribosylamine and 2-carboxamideglutacondialdehyde (see Discussion).

Evidence that the adenosine diphosphate ribose moiety is still attached to ONAD comes from its chromatographic and solubility characteristics. ONAD is insoluble in ethanol as are other adenosine derivatives. ONAD chromatographs in solvents A and B near other adenosine compounds. CGDA is soluble in ethanol and chromatographs near the front in both solvent systems, as does glutacondialdehyde, suggesting that ONAD still contains the adenosine moiety.

The following are similarities between ONAD, CGDA, and glutacondialdehyde: (a) all give a positive 2,4-dinitrophenylhydrazine test, (b) all appear as long wavelength ultraviolet light absorbing spots after chromatography in solvents A or B, and (c) all give a bright-orange color and yellow-orange fluorescence with aniline phthalate after chromatography in solvents A or B. The color develops immediately with glutacondialdehyde, but requires about 15 min with ONAD and CGDA. Maximal absorption for the unstable *p*-nitroaniline derivatives formed in HCl occurs at 440 nm for CGDA and ONAD, and at 430 nm for glutacondialdehyde. The CGDA and ONAD derivatives decay within 30 min in 5 N HCl; the glutacondialdehyde derivative is changed within 10 min in 5 N HCl, giving a λ_{max} similar to that of the presumed product, 5-(*p*-nitroanilino-*p*-nitrophenyl)-2,4-pentadienylidenium ion (Marvell and Shahidi, 1970).

The analogous 340-nm intermediate derived from nicotinamide riboside was prepared in the same manner as was ONAD. Interestingly, this intermediate was unstable compared to ONAD in that it had a half-life of 1.5 h at pH 8.2 (compared to a half-life of 14.5 h for ONAD at this same pH), and was rapidly decomposed by organic solvents.

CGDA was prepared in situ by incubating 20 mg of ONAD in 0.2 ml of 0.1 N NaOH for 1 h. The properties of CGDA are as follows: λ_{max} of 345 nm in its basic form and at 320 nm in its acidic form, with a spectroscopically measured pK of 2.9 ± 0.2. CGDA is most stable at pH 10–12 with approximate half-lives of 20 h at pH 10, 15 h at pH 11.3, 8 h at pH 7, and 70 min at pH 13. Glutacondialdehyde, likewise, is most stable at pH 11–13 (Johnson and Rumon, 1970). At pH 3 and below, CGDA is markedly labile with half-lives of 10 min at pH 3 and 1 min at pH 1.

Kinetics of Decomposition of ONAD. The rate of decomposition of ONAD at various pH values is shown in Figure 1. This pH–rate profile in the acid region and near the pK of ONAD is similar to those exhibited by ODCN (Johnson and Morrison, 1970a). The rate constants represented in Figure 1 are intercepts from plots of k_{obsd} vs. buffer concentration. General buffer catalysis is seen in the region below pH 4 with maleate buffer at pH 1.92 and with oxalate buffer at pH 1.69. The decomposition of ONAD displays decreasing rates as the acid concentration increases below $H_0 = -1$. In a plot of log ($k_{obsd} + H_0$) vs. the logarithm of the activity of water in these solutions (Bunnett, 1961a), below $H_0 = -1$ a straight-line relationship is seen with a slope, w, of +3.01 (Bunnett, 1961b).

The rate of decomposition of ONAD increases with increasing pH above pH 8, leveling off above pH 12, and subsequently declining in the pH region above 13. In the pH region between 10 and 12, buffer catalysis of the general base type was observed with the carbonate and phosphate buffers used in this region. The following catalytic coefficients were ob-

tained: carbonate, 0.014 M^{-1} min^{-1}; phosphate, 0.22 M^{-1} min^{-1}. The kinetics in five dilutions of each buffer were determined at several pH values.

In the pH region 13.7–15.4, the rate of decomposition of ONAD followed spectrally at 340 nm exhibits apparent first-order kinetics to 90% reaction. In the pH region 12.7–13.5, an intermediate is detectable by a fast followed by a slow reaction corresponding to

$$A \xrightarrow{k_1'} B \xrightarrow{k_2'} C$$

(Figure 2, circles), where A is ONAD, B is CGDA, and C is 2-hydroxynicotinaldehyde (see Discussion). The rate constants for the transformation B → C were obtained from the slower first-order reactions and are presented in Figure 1; the rate constants for the transformation A → B were obtained from the plot of log $(A - A_\infty)$ vs. time (Figure 2, triangles) after estimation of a value for A_∞ (Garrett et al., 1966; Perrin, 1963). ONAD disappearance followed at 370 nm after acid quenching gave rate constants agreeing reasonably well with those obtained for the initial fast reaction measured at 340 nm. The disappearance of ONAD followed at 370 nm measures only the disappearance of ONAD, while measurements made at 340 nm reflect the disappearance of CGDA in addition to the disappearance of ONAD.

At pH 15.7 and 16.2, kinetic determinations made at 340 nm gave first-order plots after an initial small lag period (less than 3 min). Rate constants presented in Figure 1 are taken from the latter parts of these plots. This lag may reflect the approach to equilibrium of the reaction of ONAD to CGDA prior to the formation of 2-hydroxynicotinaldehyde. Alternatively, the lag may be due to reaction of impurities which are present in ONAD, or to side reactions of ONAD, or to a combination of both of these effects.

The solid line in Figure 1 was calculated from eq 1, where $[a_{H_2O}]$ is the activity of water (Bunnett, 1961a) at $[H^+]$ below $H_0 = -1.0$. The activity of water is taken as 1 above $H_0 = -1.0$.

$$k_{obsd} = \frac{[15.2 + 0.556(H^+)][a_{H_2O}]\ min^{-1}}{\left[1 + \frac{79.4}{(H^+)}\right][(H^+) + 0.23]} + 8.0 \times 10^{-4}\ min^{-1} + \frac{188 \times 10^{-4}\ min^{-1}}{[9.04 \times 10^{-12} + (H^+)]\left[1 + \frac{1.08 \times 10^{-15}}{(H^+)}\right]} \quad (1)$$

Product Studies. Product studies were carried out in the various pH regions. Spectral scans of completed reactions from the decomposition of ONAD in the pH region below 4 and above 13 showed ONAD decomposed to a species absorbing at 340 nm. This absorption maximum shifted to 360 nm when basified to pH 12, and the solution had a blue fluorescence under long wavelength ultraviolet light, indicating that the product is 2-hydroxynicotinaldehyde.

At pH 10–12, spectral scans showed a new 345-nm absorbing species CGDA, which was formed on decomposition of ONAD. This species slowly decomposed over several days at pH 10 and overnight at pH 12. The final product of decomposition absorbed at 360 nm and was blue fluorescent under long wavelength ultraviolet light, corresponding to 2-hydroxynicotinaldehyde.

Following incubation of ONAD in 3 N HCl, pH 11.5, phosphate buffer, 0.1 and 5 N NaOH for 1 h, both thin-layer

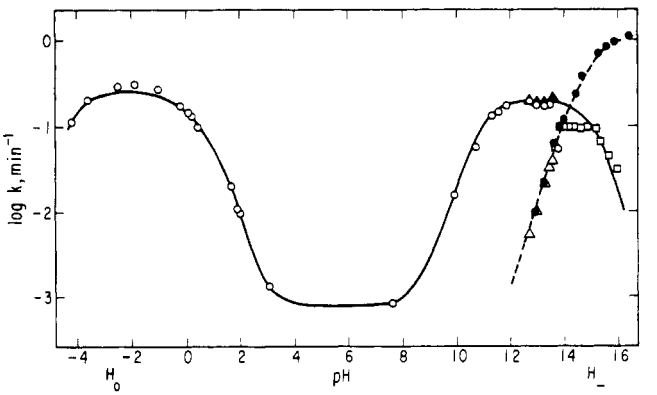

FIGURE 1: Log K_{obsd} vs. pH for the decomposition of ONAD (○, □, △, ▲) and CGDA (●) at 25 °C. (○) k_{obsd} measured at 370 nm; (□) k_{obsd} measured at 340 nm; (▲) burst reaction k measured at 340 nm; and (△) slow reaction k measured at 340 nm. Solid line calculated from eq 1 and dashed line, from eq 2. Ionic strength was maintained at 0.6 with KCl between pH 0.4 and 13.4.

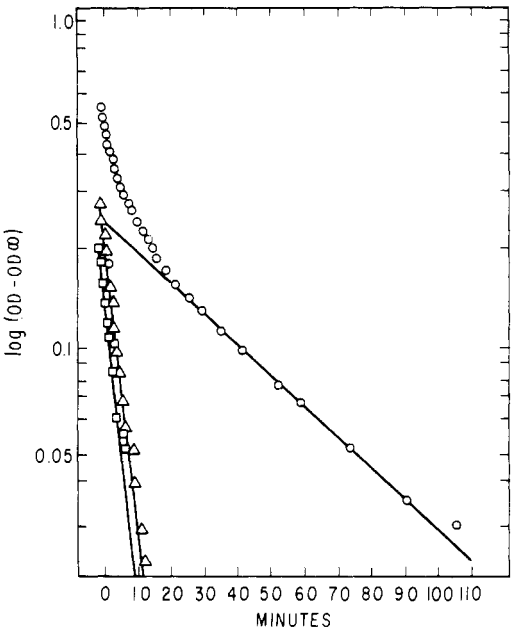

FIGURE 2: Decomposition of ONAD as a function of time measured at 25 °C in 0.2 N NaOH. Solution was initially 0.165 × 10^{-4} M in ONAD. (○) OD − OD_∞ measured at 340 nm; (△) $A - A_\infty$ calculated from OD − OD_∞ measured at 340 nm; (□) OD − OD_∞ measured at 370 nm.

analysis and enzymatic analysis for NAD^+ were performed. Analysis revealed no NAD^+ was formed in any of these pH regions. Under these conditions, NAD^+ is stable in the 3 N HCl and pH 11.5 buffers, but not in the 0.1 and 5 N NaOH buffers, where hydrolysis to nicotinamide takes place. However, chromatographic analysis revealed that no nicotinamide was formed at any of these pH values.

In the pH 11.5 phosphate and 0.1 N NaOH buffers, a new long wavelength ultraviolet light absorbing species was observed on chromatographic analysis, which has a λ_{max} of 345 nm at pH 7.0, corresponding to CGDA. Chromatography in solvent A of the four incubation mixtures showed that 2-hydroxynicotinaldehyde was formed at all pH values, and that several other unidentifiable products, in addition to the impurities initially present in ONAD, were formed. The 3 N HCl incubation mixture was observed to contain several yellow-orange fluorescent species chromatographing near the origin and a species with an R_f of 0.45. The pH 11.5 phosphate and

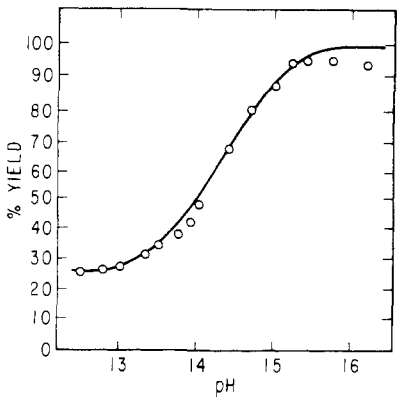

FIGURE 3: Yield of 2-hydroxynicotinaldehyde from 0.762×10^{-4} M ONAD as a function of pH, measured at 360 nm and 25 °C. (○) experimental values; solid line calculated for theoretical acid of pK_a 14.25.

0.1 N NaOH buffers contained two yellow fluorescent species of R_f 0.35 and 0.48, a species with an R_f of 0.45, and two green fluorescent species of R_f 0.60 and 0.85. The 5 N NaOH incubation mixture contained three purple fluorescent species with R_f values of 0.42, 0.55, and 0.62, and two species with an R_f of 0.35 and 0.45.

Yield of 2-Hydroxynicotinaldehyde from ONAD. The final yields of 2-hydroxynicotinaldehyde from the decomposition of ONAD in solutions of various pH are shown in Figure 3. The yield varies with pH as the titration curve of an acid with an apparent pK_a of 14.25, leveling off to a yield of about 25% below pH 13 and with a maximal yield of 95% above pH 15.

Kinetics of Decomposition of CGDA. The decomposition kinetics of CGDA, determined at pH 13–16.2, are shown in Figure 1. The rate constants increase linearly with a slope of +1.0 from pH 13 to 14.5 and finally level off above pH 15. The slower rate constants for the reaction B → C (k_2') obtained between pH 12.7 and 13.5 for the decomposition of ONAD (Figure 1) correspond very well to those obtained for the decomposition of CGDA in this pH region, indicating that ONAD decomposes to CGDA. The dashed line in Figure 1 was calculated from eq 2.

$$k_{obsd} = \frac{1.41 \times 10^{-15}\ \text{min}^{-1}}{[(H^+) + 1.27 \times 10^{-15}]} \qquad (2)$$

Kinetics of Formation of 2-Hydroxynicotinaldehyde from ONAD. In Figure 4 are shown the rate constants for formation of 2-hydroxynicotinaldehyde from ONAD. In the pH regions 12.7–13.3 and 15.2–16.2, apparent first-order plots for log ($F_\infty - F_t$) vs. time are linear to over 90% reaction. In the pH region 13.5–14.7, a plot of log ($F_\infty - F_t$) vs. time shows a small induction period before the onset of first-order kinetics. Rate constants for these pH values were taken from the apparent first-order part of the plot.

Discussion

Structure of NAD^+ Alkaline Products. Scheme III illustrates the equilibrium and rate relationships involved in the alkaline destruction of NAD^+. The properties of ONAD are consistent with the ring-opened Schiff base of 2-carboxamideglutacondialdehyde and adenosine diphosphate ribosylamide. The pK_a values of −1.90 and 11.18 can be compared with other glutacondialdehyde Schiff bases: −1.78 and 12.0 for ODCP, the ring-opened form of *N,N*-dimethylcarbamoylpyridinium ion (DCP); 9.8 for ODCN; and ~13 for the ring-opened form of 2,4-dinitrophenylpyridinium ion (Johnson and Morrison, 1970a; Johnson and Rumon, 1970; Moss, 1963).

Scheme III

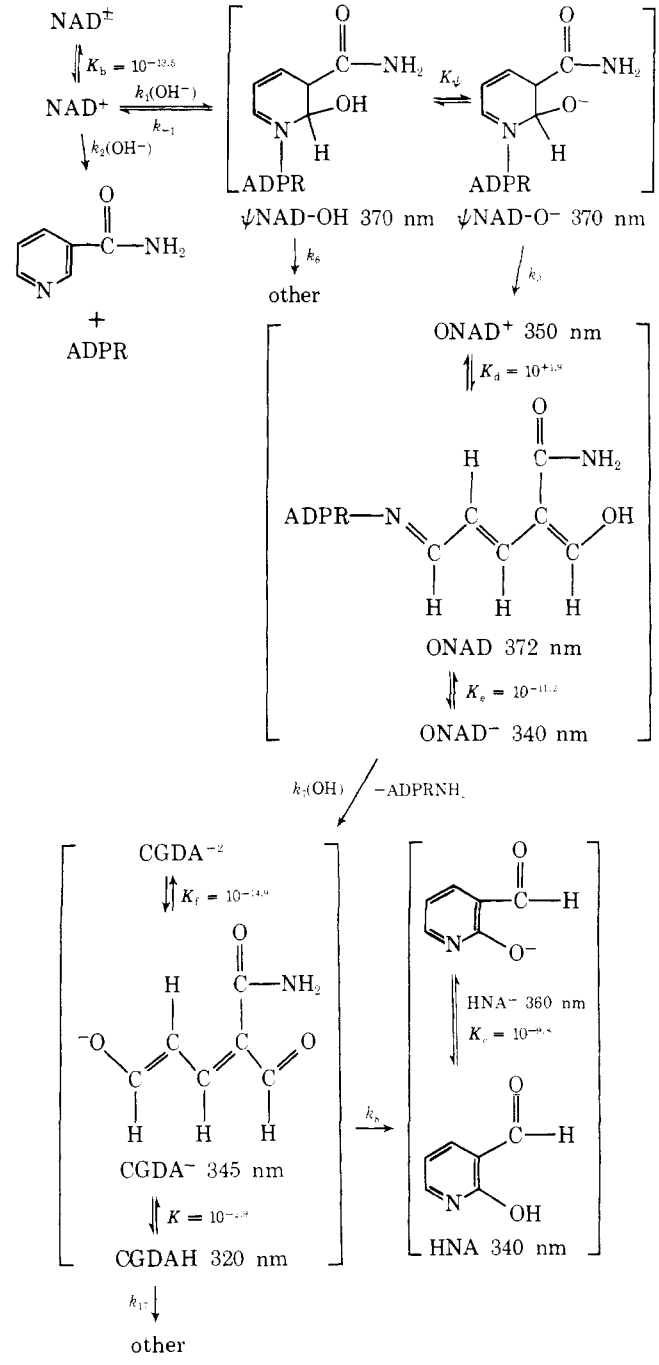

The increase of more than 1 pK_a unit of ONAD as compared to ODCN is in the direction expected, since the adenosine diphosphate ribose moiety would be less electron-withdrawing than the dimethylcarbamoyl moiety. The reactivity of ONAD towards carbonyl reagents and aniline derivatives is similar to that of ODCN and glutacondialdehyde, and its chromatographic behavior supports the Schiff base structure.

In the pH region 11–13, CGDA can be observed as an intermediate resulting from the decomposition of ONAD. The properties of CGDA are consistent with the structure of 2-carboxamideglutacondialdehyde, which would be the expected product of the Schiff base hydrolysis of ONAD. CGDA has a pK_a of 2.9, as compared to 5.75 for glutacondialdehyde (Schwarzenbach and Lutz, 1940). The decrease in pK_a is expected for the addition of the electron-withdrawing carboxamide substituent. The pK_a values of other similar structures

are as follows: α-amino-β-carboxymuconic acid ε-semialdehyde, 5.1; α-hydroxymuconic acid ε-semialdehyde, 6.4; and 5-amino-2,4-pentadienal, 3.9 (Kojima et al., 1961; Ichiyama et al., 1965; Joussot-Dubien and Hondard-Pereyre, 1969). The above related compounds all undergo shifts of their maximal absorbance to lower wavelengths on acidification to pH values below their pK_a. For example, the spectrum of CGDA (345 nm in its anionic form and 320 nm in its neutral form) resembles that of glutacondialdehyde (362 nm in its anionic form and 300 nm in its neutral form).

At pH 13–16.2, CGDA decomposes to form 2-hydroxynicotinaldehyde, which could occur by eq 3..

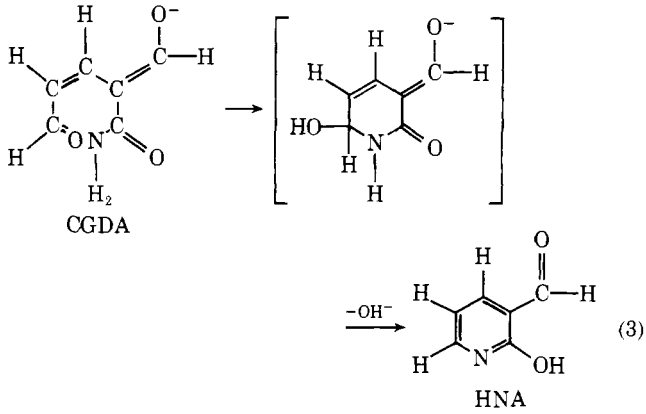

(3)

The transient 370-nm species from NAD^+, which was previously identified as the ring-opened species (Johnson and Morrison, 1970b), is the pseudobase ψNAD-OH (see Scheme III).[2] The rapid reversal to NAD^+ upon acid quenching (Johnson and Morrison, 1970b) is the behavior expected for the pseudobase structure. Analogies for the shift of maximal absorbance to longer wavelengths include 1-methyl-3,5-dicyanopyridinium ion and 1-methyl-3,4,5-tricyanopyridinium ion, which readily add hydroxide ion producing shifts in maximal absorbance from 287 to 350 nm and from 313 to 384 nm, respectively (Hanstein and Wallenfels, 1967; Wallenfels and Hanstein, 1967). The 1,2-dihydro derivatives of these compounds absorb at 389 and ~440 nm, respectively. The 1,2-dihydro derivative of NAD^+ absorbs at 395 nm (Chaykin and Meissner, 1964). The spectral shift seen when OH is substituted for H with these two compounds resembles that obtained when the 370-nm intermediate of NAD^+ is compared to the 1,2-dihydro-NAD^+ derivative.

The formation of the pseudobase ψNAD-OH would be expected to be first-order in hydroxide ion. The increasing effectiveness of this reaction with increasing pH (Johnson and Morrison, 1970a) compared to the cleavage of the nicotinamide-ribose bond and ionization of the amide group of NAD^+, which are also first-order in hydroxide ion (Anderson and Anderson, 1963), can be explained by the ionization of ψNAD-OH to its anionic form, which also absorbs maximally at 370 nm. An analogous case is the tetrahedral intermediate resulting from addition of hydroxide ion to diphenylimidazolinium chloride, which has a pK_a of 12.74 with both the neutral and anionic forms absorbing maximally at the same wavelength (Robinson, 1968). Ionization constants of pseudobases of various substituted *N*-cyano- and *N*-methylquinolinium ions have K_a values ranging from 10^{-10} to 10^{-15} (Cooksey and Johnson, 1968).

Hydrolysis of ONAD in Acid. The dependence of the rate of decomposition of ONAD at pH values below 3 can be explained by eq 4 through 7, for acid-catalyzed Schiff base hydrolysis.

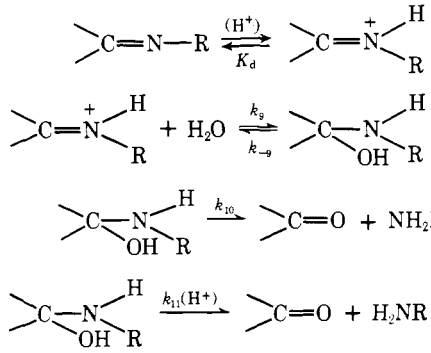

(4)

(5)

(6)

(7)

The steady-state rate (eq 8) can be derived for this sequence of reactions. This scheme includes decomposition of the protonated amino alcohol intermediate (eq 7), as well as decomposition of the zwitterionic form (eq 6).

$$k_{obsd} = \frac{k_9[k_{10} + k_{11}(H^+)]}{\left[1 + \frac{K_d}{(H^+)}\right][k_{10} + (k_{-9} + k_{11})(H^+)]} \quad (8)$$

Decomposition of protonated carbinolamines derived from weakly basic amines can take place in addition to decomposition of the zwitterionic form, an example of which is the hydrolysis of *N*-*p*-chlorobenzylidene aniline (Cordes and Jencks, 1962). The electron-withdrawing groups on the amino nitrogen permit amine expulsion with less driving force as compared to carbinolamines derived from more basic amines, which require the zwitterionic form for reaction (Jencks, 1969).

At pH values above 1 where $k_{10} > k_{11} \times (H^+)$ and $(k_{-9} + k_{11}) \times (H^+)$, eq 8 reduces to eq 9. The value of k_9, which best fits the data, is 66.1 min^{-1}. A water term, k_w, equal to 8×10^{-4} min^{-1}, is included in order to fit the data in Figure 1. The general catalysis found in this pH region is to be expected for hydrolysis of a Schiff base (Jencks, 1969). At pH < 1 values of 0.23 for $k_{10}/(k_{-9} + k_{11})$ and 8.4×10^{-3} for $k_{11}/(k_{-9} + k_{11})$ were obtained by solving eq 8 at several data points.

$$k_{obsd} = \frac{k_9}{\left[1 + \frac{K_d}{(H^+)}\right]} \quad (9)$$

The rate constants decrease below $H_0 = -1.0$ and give a slope, *w*, of +3.01 when $\log (k_{obsd} + H_0)$ is plotted vs. $\log a_{H_2O}$. It has been proposed that the value of *w* can be used to indicate the role of water in acid-catalyzed reactions (Bunnett, 1961b). For $+1.2 < w < +3.3$, water is considered to act as a nucleophile. A decrease in the activity of water in eq 5 would reduce the concentration of carbinolamine intermediate produced, which would reduce the overall rate of hydrolysis resulting from eq 6 and 7. In the hydrolysis of *p*-chlorobenzylidineaniline, a decrease in the rate of hydrolysis was seen at increasing acid concentrations (Cordes and Jencks, 1962). This was attributed to the participation of water as a nucleophile and as a proton-transfer agent.

Equation 8 was modified to include the participation of water, resulting in eq 10 after rearrangement. Equation 10 was used to calculate the acid limb in Figure 1 using the values obtained for $k_{10}/(k_{-9} + k_{11})$ and $k_{11}/(k_{-9} + k_{11})$, k_9 and K_d

[2] pK_{a1} and pK_{a2} are equivalent to pK_d and pK_e of Scheme III; k_H is equivalent to k_9. The structure shown for ψNAD-OH is the 2-hydroxy isomer, which is presumed to be in equilibrium with the 4-hydroxy isomer.

+ $10^{1.9}$. The values for a_{H_2O} were taken from Bunnett (1961a).

$$k_{obsd} = \frac{\left[\frac{k_9k_{10}}{(k_{-9}+k_{11})} + \frac{k_9k_{11}(H^+)}{(k_{-9}+k_{11})}\right](a_{H_2O})}{\left[1+\frac{K_d}{(H^+)}\right]\left[(H^+)+\frac{k_{10}}{(k_{-9}+k_{11})}\right]} \quad (10)$$

In Table II are given the experimental values for $k_H(k_9)$, K_{a1}, K_{a2}, and k_H/K_{a2} of ODCN, ODCP, and ONAD, for comparative purposes.[2] From a comparison of the values for k_H, it can be seen that the rate constant estimated for ODCN is only two- to sevenfold larger than that obtained for ONAD. Therefore, the effect of substituting a ribosyl derivative for the dimethylcarbamoyl moiety on the imino nitrogen of ODCN is small. Comparison of the k_H values of ODCN and ODCP shows that the 3-carboxamide substituent increases k_H by 25- to 100-fold. The electron-withdrawing 3-carboxamide group would be expected to increase the rate of hydrolysis of ODCN compared to ODCP.

Hydrolysis of ONAD at Intermediate pH. The pH–rate maxima at intermediate pH values observed for ODCP and ODCN have been explained by a return of ODCP to DCP and ODCN to DCN, respectively, followed by hydrolysis of DCP and DCN at the carbamoylheterocyclic nitrogen atom (Johnson and Morrison, 1970a; Johnson and Rumon, 1970). However, the pH–rate maximum observed for the decomposition of ONAD at alkaline pH values cannot be explained in this manner. A search for the formation of NAD^+ or for nicotinamide, its hydrolysis product, revealed that neither was formed in this pH region.

The bell-shaped pH–rate maximum in the decomposition of ONAD can be explained by a change in rate-determining step from rate-limiting attack of hydroxide ion at pH values below 13 to rate-limiting expulsion of amine at pH values above 13. The leveling off of the rate constants at pH 11–13 is due to ionization of ONAD, which reduces the amount of neutral Schiff base present. The opposing effects of increasing hydroxide ion and decreasing concentration of neutral Schiff base produce a net pH-independent reaction. Equations 11 through 13 describe this behavior.

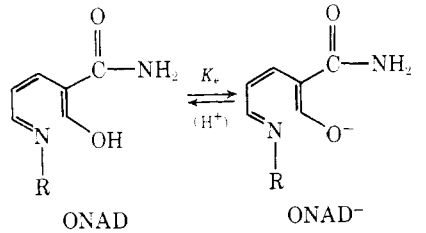

(11)

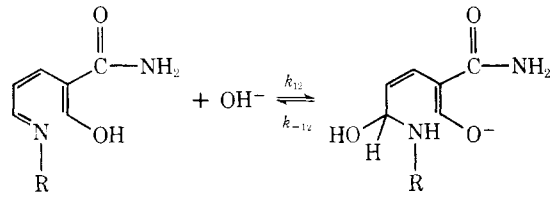

(12)

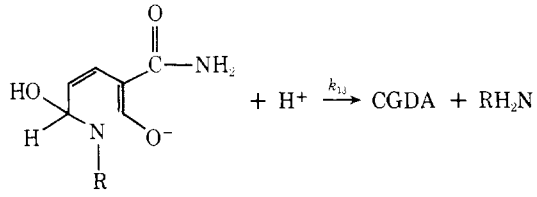

(13)

TABLE II: Rate and Equilibrium Constants for Hydrolysis of Glutacondialdehyde Schiff Bases.

Constant[d]	ODCN[a]	ODCP[b]	ONAD
K_{a1}	1.59×10^{-10} M	1×10^{-12} M	6.6×10^{-12} M
K_{a2}	$2\text{–}10 \times 10^{3}$ M[c]	60.3 M	7.94×10^{1} M
k_H/K_{a2}	4.28×10^{-1} M^{-1} min^{-1}	6×10^{-2} M^{-1} min^{-1}	0.833×10^{-1} M^{-1} min^{-1}
k_H	86–430 min^{-1} [c]	3.61 min^{-1}	66.1 min^{-1}

[a] From Johnson and Morrison, 1970a. [b] From Johnson and Rumon, 1970. [c] Estimated from the ΔpK observed for ODCP and ONAD. [d] K_{a1} is equivalent to K_e and K_{a2} is equivalent to K_d in Scheme III; k_H is equivalent to k_9.

The steady-state eq 14 can be derived for eq 11 through 13.

$$k_{obsd} = \frac{\frac{k_{12}k_{13}K_w(H^+)}{k_{-12}}}{[(H^+)+K_e]\left[1+\frac{k_{13}(H^+)}{k_{-12}}\right]} \quad (14)$$

$$k_{obsd} = \frac{k_{12}K_w}{[(H^+)+K_e]} \quad (15)$$

At pH values below 12 where $(k_{13}/k_{-12})(H^+) > 1$, eq 14 reduces to eq 15. A plot of $1/k_{obsd}$ vs. (H^+) would be expected to give $1/k_{12}K_w$ as the slope and K_e/K_wk_{12} as the intercept. A straight-line relationship was observed and values for k_{12} = 188 min^{-1} and $K_e = 9.04 \times 10^{-12}$ M were obtained. The pK value of 11.04 obtained kinetically is in good agreement with the value of 11.18 obtained spectrally.

Hydrolysis of ONAD at High pH. At pH values above 13, where $K_e > (H^+)$ and $1 > (k_{13}/k_{-12})(H^+)$, eq 14 reduces to eq 16.

$$k_{obsd} = \frac{k_{12}k_{13}K_w(H^+)}{k_{-12}K_e} \quad (16)$$

The value for k_{13}/k_{-12} which best fits the data is 1.08×10^{-15}. The deviation of the apparent first-order rate constants at pH 13.7–14.5 from the theoretical curve in the basic limb of Figure 1 (calculated from eq 14 using the values obtained for k_{12}, K_e, and k_{13}/k_{-12}) result from the consecutive reactions ONAD → CGDA → 2-hydroxynicotinaldehyde. The experimental rate constants are not true first-order rate constants for the decomposition of ONAD but are complex constants reflecting the consecutive decay of ONAD to CGDA and the cyclization of CGDA to form 2-hydroxynicotinaldehyde.

The pH–rate profile for the decomposition of CGDA has a slope of +1.0 from pH 13–14.5. Above pH 15, the rate constants level off. This is consistent with intramolecular hydroxide ion catalyzed attack of the amide group on the terminal aldehyde group, because above this pH the amide group is completely in its ionized form. Equations 17 and 18 describe this behavior from which steady-state eq 19 can be derived.

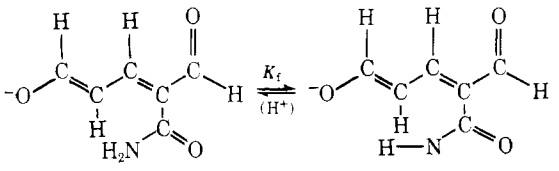

(17)

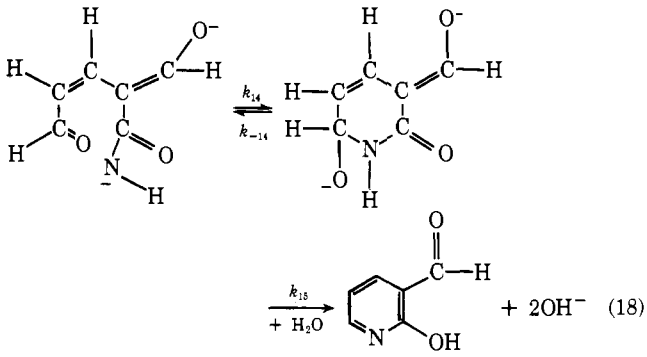

$$k_{obsd} = \frac{k_{14}k_{15}K_f}{[k_{-14} + k_{15}][(H^+) + K_f]} \quad (19)$$

The anionic ureido group is known to be an effective nucleophile in intramolecular condensation reactions with carbonyl groups (Taylor, 1968; Hegarty and Bruice, 1969), and such a reaction (eq 18) would be expected here.

A plot of $1/k_{obsd}$ vs. (H^+) would be expected to give $(k_{-14} + k_{15})/k_{14}k_{15}$ as the intercept and $(k_{-14} + k_{15})/K_f k_{14}k_{15}$ as the slope. A straight-line relationship was obtained and values for $k_{14}k_{15}/(k_{-14} + k_{15}) = 1.1$ min^{-1} and $K_f = 1.27 \times 10^{-15}$ M were obtained. The dashed line in Figure 1 was calculated using these experimentally obtained results. The K_f value of 1.27×10^{-15} M is in the range expected for an amide group (Tarvainen and Koskikallio, 1970).

The bell-shaped curve for formation of 2-hydroxynicotinaldehyde from ONAD (Figure 4) can be explained by the consecutive reactions in Scheme III. At pH 13.0–13.8, the rate-limiting step for formation of 2-hydroxynicotinaldehyde from ONAD is the cyclization of CGDA. At pH values above 15, the hydrolysis of ONAD to CGDA becomes rate limiting. At intermediate pH values, the observed rate of formation of 2-hydroxynicotinaldehyde depends on both reactions. The dashed line of Figure 4 below pH 14 is the theoretical curve calculated from eq 19 for the cyclization of CGDA; the solid line above pH 14 is the theoretical curve calculated from eq 14 for the hydrolysis of ONAD. The dashed and solid lines of Figure 1 correspond well with Figure 4.

Yield of 2-Hydroxynicotinaldehyde. Further support for a change in rate-limiting step in the formation of 2-hydroxynicotinaldehyde comes from a consideration of the variation in yield of 2-hydroxynicotinaldehyde. The yield of 2-hydroxynicotinaldehyde varies with pH as the titration curve of an acid with an apparent pK_a of 14.25. The bell-shaped pH–rate profile for formation of 2-hydroxynicotinaldehyde cannot be accounted for by this pK_a value. This means that the rate-limiting and product-forming steps are not identical. At pH 14, the cyclization of CGDA to form 2-hydroxynicotinaldehyde is rate limiting. Above pH 15, the hydrolysis of ONAD to CGDA is rate limiting. Below pH 15, CGDA is partitioned between hydroxide ion catalyzed ring closure to form 2-hydroxynicotinaldehyde and an uncatalyzed reaction to form other products. A water term for ring closure of CGDA is included to account for the leveling off to a yield of 25% at pH 13. Above pH 15, the amide group of CGDA is completely ionized and 2-hydroxynicotinaldehyde is the major product in yields of 95%. Equation 20 holds for Scheme IV. From this relationship, eq 21 can be obtained, which describes the dependence of the yield of 2-hydroxynicotinaldehyde on hydroxide-ion concentration. At high hydroxide ion concentration, k_{16} is small compared to $k_8K_f(OH^-)/K_w$ and eq 21 becomes eq 22. At low hydroxide ion concentration, $k_{16} > k_8K_f(OH^-)/K_w$, resulting in eq 23.

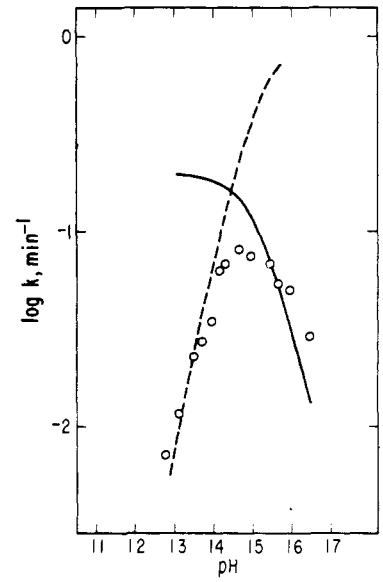

FIGURE 4: Log k_{obsd} for formation of 2-hydroxynicotinaldehyde from ONAD as a function of pH, followed by emission at 460 nm after excitation at 350 nm. (○) Experimental values; solid line calculated from eq 14; dashed line calculated from eq 19.

Scheme IV

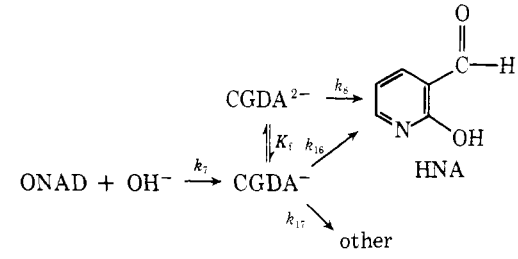

A plot of 100/HNA vs. $1/(OH^-)$ gave an initially straight line with an intercept of 1.0 at $1/(OH^-) = 0$ and slope = 1.05 $= k_{17}K_w/k_8K_f$. At higher values for $1/(OH^-)$, the line levels off to $k_{17}/k_{16} = 3.1$.

$$\frac{\%HNA}{100 - \%HNA} = \frac{k_8K_f(OH^-)/K_w + k_{16}}{k_{17}} \quad (20)$$

$$\frac{100}{\%HNA} = 1 + \frac{k_{17}}{K_f k_8(OH^-)/K_w + k_{16}} \quad (21)$$

Equation 21 can be rearranged to eq 22. Substituting $(OH^-) = K_w/K_{app}$,

$$\frac{100}{\%HNA} = \frac{K_f k_8(OH^-)/K_w + k_{16} + k_{17}}{K_f k_8(OH^-)/K_w + k_{16}} \quad (22)$$

where K_{app} is the apparent ionization constant for the plot of percent yield of 2-hydroxynicotinaldehyde vs. pH (Figure 3), eq 23 results, since 100%/HNA = 100/62.3 at the midpoint of the curve.

$$K_{app} = \frac{k_8K_f}{1.65\,k_{17} - k_{16}} \quad (23)$$

Equation 23 shows that the apparent ionization constant of $10^{-14.25}$ for formation of 2-hydroxynicotinaldehyde is a result of the partitioning of CGDA between other products and 2-hydroxynicotinaldehyde and is dependent upon K_f, the true ionization constant of CGDA, which is equal to $10^{-14.9}$.

A comparison of the rate constants for formation of 2-hydroxynicotinaldehyde from NAD$^+$ and ONAD shows that

the rate constants agree reasonably well, indicating the rate-limiting step for formation of 2-hydroxynicotinaldehyde from NAD^+ is the decomposition of ONAD. The formation of ψNAD-OH from NAD^+ and its subsequent decomposition of ONAD are rapid compared to the decomposition of ONAD to CGDA, which then cyclizes to form 2-hydroxynicotinaldehyde.

The initial burst in fluorescence seen in the formation of 2-hydroxynicotinaldehyde from NAD^+ is probably due to the occurrence of side reactions of CGDA, as indicated in Schemes III and IV. The rate constants for this initial burst reaction are similar to those for the formation of ONAD from NAD^+ (see Table I). Pseudobases of 1-substituted pyridines have been postulated to undergo disproportionation to 2-pyridones and 2-hydroxytetrahydropyridines (Decker, 1892, 1903), which remains a possibility here.

Acknowledgment

We are grateful to Mrs. Beatrice Goodman for typing the manuscript.

References

Adams, M. J., Buehner, M., Chandrasekhar, K., Ford, G. C., Hackert, M. L., Anders, L., Rossman, M. G., Smiley, I. E., Allison, W. S., Everse, J., Kaplan, N. O., and Taylor, S. S. (1973), *Proc. Natl. Acad. Sci. U.S.A. 70,* 1968.

Anderson, B. M., and Anderson, C. D. (1963), *J. Biol. Chem. 238,* 1475.

Arnold, L. J., Jr., and Kaplan, N. O. (1974), *J. Biol. Chem. 249,* 6521.

Buehner, M., Ford, G. C., Moras, D., Olsen, K. W., and Rossman, M. G. (1974), *J. Mol. Biol. 90,* 25.

Bunnett, J. F. (1961a), *J. Am. Chem. Soc. 83,* 4968.

Bunnett, J. F. (1961b), *J. Am. Chem. Soc. 83,* 4956.

Chaykin, S., and Meissner, L. (1964), *Biochem. Biophys. Res. Commun. 14,* 233.

Cooksey, C. J., and Johnson, M. D. (1968), *J. Chem. Soc. B,* 1191.

Cordes, E. H., and Jencks, W. P. (1962), *J. Am. Chem. Soc. 84,* 832.

Decker, H. (1892), *Chem. Ber. 25,* 3326.

Decker, H. (1903), *Chem. Ber. 36,* 2568.

Everse, J., Barnett, R. E., Thorne, C. J. R., and Kaplan, N. O. (1971), *Arch. Biochem. Biophys. 143,* 444.

Freytag, H., and Nendert, W. (1932), *J. Prakt. Chem. 135,* 15.

Fromm, H. J. (1961), *Biochim. Biophys. Acta 52,* 199.

Garrett, E. R., Seydel, J. K., and Sharpen, A. J. (1966), *J. Org. Chem. 31,* 2219.

Gerlach, D., Pfleiderer, G., and Holbrook, J. J. (1965), *Biochem. Z. 343,* 354.

Guilbert, C. C., and Johnson, S. L. (1970), *Biochemistry 10,* 2313.

Hanstein, W., and Wallenfels, K. (1967), *Tetrahedron 23,* 585.

Hegarty, A. F., and Bruice, T. C. (1969), *J. Am. Chem. Soc. 91,* 4924.

Ichiyama, A., Nakamura, S., Kawai, H., Honjo, T., Nishizuka, Y., Hayaishi, O., and Senoh, J. (1965), *J. Biol. Chem. 240,* 740.

Jencks, W. P. (1964), *Prog. Phys. Org. Chem. 2.*

Jencks, W. P. (1969), Catalysis in Chemistry and Enzymology, New York, N.Y., McGraw Hill Publishing Co., Chapter 10.

Johnson, S. L., and Morrison, D. L. (1970a), *Biochemistry, 9,* 1460.

Johnson, S. L., and Morrison, D. L. (1970b), *J. Biol. Chem. 245,* 4519.

Johnson, S. L., and Rumon, K. A. (1970), *Biochemistry, 9,* 847.

Joussot-Dubien, J., and Hondard-Pereyre, J. (1969), *Bull. Soc. Chim. Fr.,* 2619.

Kaplan, N. O., Ciotti, M. M., and Stolzenbach, F. E. (1954), *J. Biol. Chem. 211,* 431.

Kaplan, N. O., Colowick, S. P., and Barnes, C. C. (1951), *J. Biol. Chem. 191,* 461.

Kaplan, N. O., and Everse, J. (1972), *Adv. Enzyme Regul. 10,* 323.

Klingenberg, M. (1965), in Methods of Enzymatic Analysis, Bergmeyer, H. U., Ed., Vol. 2, New York, N.Y., Academic Press, p 528.

Kojima, Y., Itada, N., and Hayaishi, O. (1961), *J. Biol. Chem. 236,* 2223.

Kosower, E. M. (1962), Molecular Biochemistry, New York, N.Y., McGraw-Hill, p. 194.

Lowry, O. H., Passonneau, J. V., and Rock, M. K. (1961), *J. Biol. Chem. 236,* 2756.

Marvell, E. N., and Shahidi, I. (1970), *J. Am. Chem. Soc. 92,* 5646.

Moss, E. K. (1963), Ph.D. Thesis, University of Arizona, Tucson, Arizona.

Paul, M. A., and Long, F. A. (1957), *Chem. Rev. 57,* 1.

Perrin, D. D. (1963), *J. Chem. Soc.,* 1284.

Racker, E., and Krimsky, I. (1952), *J. Biol. Chem. 198,* 731.

Robinson, D. D. (1968), *Tetrahedron Lett. 48,* 5007.

Schwarzenbach, G., and Lutz, K. (1940), *Helv. Chim. Acta 23,* 1147.

Tarvainen, I., and Koskikallio, J. (1970), *Acta Chem. Scand. 24,* 1129.

Taylor, P. J. (1968), *J. Chem. Soc. B.* 1554.

Van Eys, J., Stolzenbach, F. E., Sherwood, L., and Kaplan, N. O. (1958), *Biochim. Biophys. Acta 27,* 63.

Vestling, C. S., and Kunsch, U. (1968), *Arch. Biochem. Biophys. 127,* 568.

Wallenfels, K., and Hanstein, W. (1967), *Justus Liebigs Ann. Chem. 709,* 151.

Yagil, G. (1967), *J. Phys. Chem. 71,* 1034.